Contouring by Moiré Interferometry

by Y.Z. Dai and F.P. Chiang

ABSTRACT—A double-exposure moiré-interferometry technique for topographic contour measurement of an arbitrarily curved object is presented. A curved surface coated with light-sensitive material is exposed twice in a volume of virtual gratings formed by the interference of two coherent light beams split from a laser. An adequate rotation of the curved surface relative to the virtual grating between the two exposures produces moiré fringes which reveal topographic contour, or contour under some conditions, of the surface. The advantage of the present method in comparison with others is that it offers both reasonably good fringe quality and easily adjustable high sensitivity. The sensitivity of the technique is shown to be from the order of micrometer to that of millimeter depending on the frequency of the virtual grating and the amount of the relative rotation. This technique was successfully applied to the topographic contour measurement of a cylindrical shell with and without a diametrical point loading.

The principle of this paper and some early results were presented at the SPIE conference held at Dearborn, MI on June 27-30, 1988 and appeared in its proceedings.[1]

Introduction

Some of the existing methods for measuring topographic contours include the shadow moiré method,[2,3] the projection moiré method,[4] the holographic method[5] and the laser-speckle method.[6] The main disadvantage of shadow and projection moiré methods is the lack of sensitivity; of the holographic method, the sophisticated optical arrangement; of the laser-speckle method, the poor fringe quality. In the present work, a double-exposure moiré-interferometry technique is described for topographic contour measurement which offers both high sensitivity and good fringe quality.

Moiré interferometry[7] as a highly sensitive displacement measuring method is widely used in experimental-mechanics research. However, it has been limited so far to in-plane problems except when it is combined with the holographic method.[8,9] The disadvantage of such a combination is twofold: First, it makes the corresponding optical arrangement very sophisticated; Secondly, it cannot offer good quality fringes compared with those by classic moiré or moiré interferometry methods because of the speckle effect. This drawback can be overcome by the present technique which shall be called 'Double-exposure Moiré Interferometry' in the following discussion.

Like any other moiré method, double-exposure moiré interferometry also needs two sets of gratings to form moiré fringes. These two sets of gratings are all formed on a specimen surface, which is coated with a light sensitive medium, by exposing the specimen to a volume of virtual gratings formed by the interference between two intersecting coherent light beams split from a laser. If the specimen rotates an adequate angle relative to the virtual grating between the two exposures, then the two sets of gratings formed on the specimen surface will interfere to form moiré fringes which reveal the topographic contour of the object. Specimen deformation between the exposures will produce moiré fringes too, making the deformation also measurable by this technique.

The scope of this paper will include discussion on the fringe-forming mechanism; topography-evaluating method; the sensitivity and range of measurement; the condition under which this method provides contour; and some experimental demonstrations.

Fringe-forming Mechanism

When two collimated coherent light beams split from a laser meet in space as shown in Fig. 1, they interfere constructively and destructively such that the light-intensity distribution is uniform in planes with surface normals in the plane formed by these two beams and perpendicular to line $\overline{OC}$. Therefore, a volume of dark and light sheets in the common space of those two beams is formed and called a virtual grating which will cast gratings on any objects in the volume. According to the geometry shown, the pitch p of such a grating in an arbitrary plane π is

$$p = \frac{\lambda}{\sin i_A + \sin i_B} \tag{1}$$

or

$$p = \frac{\lambda}{2 \sin \alpha \cos \theta} \tag{2}$$

where p is the grating pitch in the π plane, λ is the wavelength of the illuminating light source; α is half the

Y.Z. Dai (SEM Member) is Graduate Student and F.P. Chiang (SEM Fellow) is Professor, State University of New York at Stony Brook, Department of Mechanical Engineering, Stony Brook, NY 11794-2300.

Original manuscript submitted: November 11, 1989. Final manuscript received: January 10, 1991.

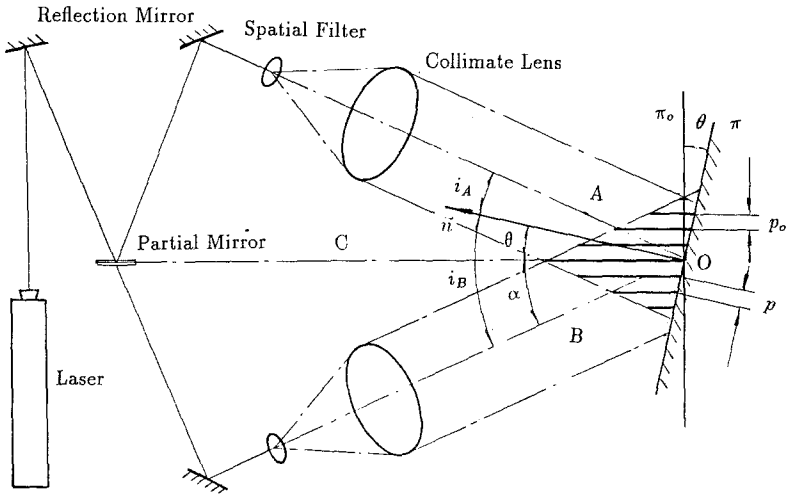

Fig. 1—An optical configuration for moiré interferometry

illuminating angle between the two light beams; and θ is the angle between the normal direction of the specimen surface and the bisectional direction $\overline{OC}$ of the two light beams. When $\theta = 0$, which corresponds to symmetric illumination ($i_A = i_B = \alpha$), we have

$$p = p_o = \frac{\lambda}{2 \sin \alpha} \tag{3}$$

where p_o is the grating pitch in the π_o plane (surface normal $\overline{OC}$) and it is a constant once the optical system is fixed. Equation (2) can be simplified by utilizing the relation given by eq (3), yielding

$$p = \frac{p_o}{\cos \theta} \tag{4}$$

The corresponding grating frequency is

$$f = \frac{1}{p} = \frac{\cos \theta}{p_o} \tag{5}$$

Equations (4) and (5) show that grating pitch p and frequency f in the π plane will change as a function of angle θ, indicating that two sets of gratings with a different number of gratings could be registered on a certain region of an object if there is a change in θ between the two gratings' registration. The change in θ could be due to a rotation of the specimen relative to the virtual grating.

If a curved surface coated with a light-sensitive medium undergoes the same procedure, then the two sets of gratings will interfere to form a fringe pattern on the specimen surface. This fringe pattern reveals the surface topographic contour via some mathematical expressions which shall be derived in the later sessions. This is the principle of topographic contour measurement by double-exposure moiré interferometry.

Measurement of Uniform Deformation

Double-exposure moiré interferometry may be used for the measurement of uniform radial expansion or shrinkage of cylindrical surfaces even without any rotation between the two exposures. A cylindrical surface is exposed to the virtual grating as shown in Fig. 2. Suppose there are n gratings formed on arc $\hat{cf}$. Then, for some reason, the

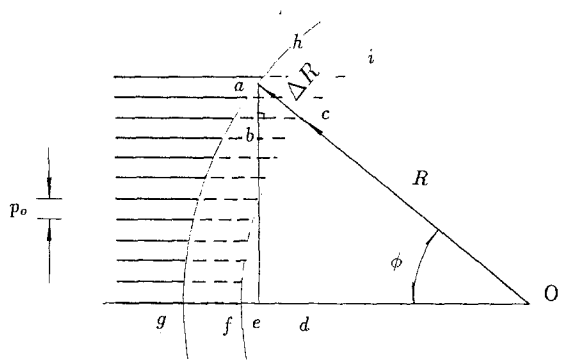

Fig. 2—Uniform radial expansion of a cylindrical shell

shell expands from $\hat{fci}$ to $\hat{gah}$ with point f moving to g and point c to a. Because of the expansion, arc $\hat{fc}$ which has already been exposed to a total number of n gratings now is expanded to arc $\hat{ga}$ and becomes capable of registering a total number of m gratings. The difference in grating numbers will create fringes which are related to the amount of shell expansion.

Obviously, the grating pitch on the shell surface is a function of angle θ. However, the projection of surface-grating pitch on the vertical line $\overline{ea}$ is the same, i.e., pitch p_o. By following a similar analysis as that for the shadow-moiré technique,[10] we can write the number of fringes formed on arc $\hat{ga}$ as

$$Np_o = mp_o - np_o = \overline{ea} - \overline{dc} = \Delta R \sin \phi \tag{6}$$

Dividing both sides of the above equation by $\sin \phi$ yields

$$\Delta R = \frac{Np_o}{\sin \phi} \tag{7}$$

At a given point a, p_o is a constant and N can be determined by the fringe pattern obtained. In order to evaluate ΔR, we must know the value of ϕ which depends on how the fringe pattern is being recorded. If the optical axis of the recording lens coincides with line gdO, then arc $\hat{ga}$ is recorded as line $\overline{ea}$ which is defined as x. The following

relation exists

$$\sin \phi = \frac{x}{R + \Delta R} \tag{8}$$

Solving for ΔR from the above two equations, we get

$$\Delta R = \frac{RNp_o}{x - Np_o} \tag{9}$$

For the case of uniform shell shrinkage, the initial radius is $R = \overline{Oa}$, $x = \overline{dc}$ and $\sin \phi = x/R$. Substitute these into eq (7), we get

$$\Delta R = \frac{NRp_o}{x} \tag{10}$$

N in eqs (9) and (10) is ordered in such a way that it is zero when $x = 0$ and it increases for shell expansion while decreases for shrinkage, making ΔR bear the right sign. To evaluate ΔR, one just has to choose a fringe, number it, measure its x coordinate, then substitute them along with the values of R and p_o into eq (10).

Because x can be almost as large as R and N can be as small as one, ΔR has nearly the same magnitude as that of pitch p_o. While the magnitude of the latter can be as small as that of the wavelength of the illuminating light source indicating that the sensitivity of this method is quite high. The lower limit of sensitivity of this technique depends on the requirements on the density of fringes and the radius of the shell. Suppose $N/x = 10$ (fringe spacing is 0.1 mm) and $R = 100$ mm, then the lower limit is $1000p_o$. Noting that the value of p_o is generally about one micrometer, the measurable shell radial deformation range is approximately between one micrometer to one millimeter.

The above derivation was made under the condition that the fringe pattern was recorded when the shell is at the deformed state. The same analyzing method can also be applied to the case that the fringe pattern is recorded when the shell has resumed its original dimension after the two exposures, only to yield slightly different expressions.

Measurement of Surface Topography

Double-exposure moiré interferometry can be used directly for measuring topographic contour. A specimen coated with photosensitive material is first exposed to a volume of virtual grating and then it is exposed to the same virtual grating again after either the optical system or the specimen is rotated a certain angle. These two exposures will make two sets of gratings on the specimen surface. They will in general interfere with each other to form a moiré fringe pattern which is related to the topography of the specimen through certain mathematical expressions.

The form of such expressions depends on the way the optical system or specimen is rotated and the setup of the coordinate system. Three cases and the corresponding topography-evaluation expressions will be studied in the coming sessions followed by a discussion.

Rotating the Optical System

Suppose the optical system is rotated clockwise an angle α in the X - W plane (Fig. 3) between the two exposures. Without losing generality, point e is chosen to be the origin of the coordinate system and a is the point of interest. Using the conventional moiré fringe analyzing method and denoting np_o by x, we get

$$Np_o = mp_o - np_o = x \cos \alpha + w \sin \alpha - x \tag{11}$$

Solving eq (11) for w,

$$w = \frac{Np_o + x(1 - \cos \alpha)}{\sin \alpha} \tag{12}$$

where N is the fringe order at point a and it is zero when $x = w = 0$.

Applying the same analysis for the left part of the X axis, we get the following expression.

$$w = \frac{Np_o - x(1 - \cos \alpha)}{\sin \alpha} \tag{13}$$

Note that x is the length of mp_o and should be positive for both sides of the X axis. We conclude that the w evaluation expression is slightly different for the different sides of the X axis. This difference can be negligible because the term $x(1 - \cos \alpha)$ is very small compared with Np_o for small α, making the fringes represent contours of equal w coordinates, which will be discussed later.

If the fringe pattern is recorded via a lens with its optical axis coinciding with the W axis, then x in the above expressions can be measured from the photographed fringe pattern. The values of p_o and α are also known from the optical setup and the amount of rotation. Therefore, w can be evaluated.

For the case that the optical system rotates counterclockwise, the w evaluation expressions will be the same as eqs (12) and (13) except that the sign of the term $x(1 - \cos \alpha)$ will be just the opposite.

Rotating the Specimen

More often than not, it is easier to rotate a specimen rather than the optical system between the two exposures. Because of the nature of relative motion, we do expect to see the same expressions as eqs (12) and (13). However, we will go through the derivation for rotating a specimen about an arbitrary point in the following discussion.

Curve $\overset{\frown}{abc}$ on an arbitrary object rotates an angle α counterclockwise about point O to $\overset{\frown}{a'b'c'}$ as shown in Fig. 4. The difference in grating numbers yields the following relation.

$$Np_o = mp_o - np_o = x - \overline{cb} \sin (\theta - \alpha) \tag{14}$$

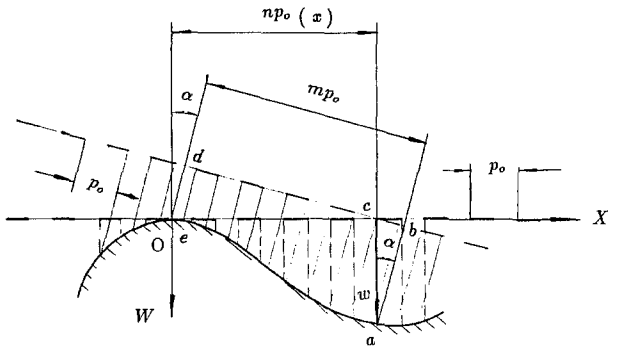

Fig. 3—Rotating the optical system

Noting that $\sin(\theta-\alpha) = \sin\theta\cos\alpha - \cos\theta\sin\alpha$; $\overline{cb} = \overline{c'b'}$, and $cb\sin\theta = x$, $\overline{cb}\cos\theta = w$, we can rewrite eq (14) as

$$w = \frac{Np_0 - x(1-\cos\alpha)}{\sin\alpha} \tag{15}$$

The term $x(1-\cos\alpha)$ bears a negative sign because the rotation of the specimen is counterclockwise and the coordinate system is fixed at the final position of the object (Fig. 4). If we change the direction of rotation or the side of the X axis under investigation, we shall get the same result as that discussed in the previous sessions.

The fact that the expressions derived for the general case are the same as those for special cases indicates that the rotating object and its center of rotation have no effect on the evaluation of topography. While the rotating direction or the change in the part of the X axis will only change the sign of a term in the expression.

Using a Periphery Camera

So far only the conventional camera has been utilized for fringe-pattern recording. The disadvantages of using such a camera for fringe-pattern recording on a curved surface is that not all points could be focused sharply because w and hence the objective distance changes from point to point making the determination of the x coordinate erroneous. Besides, w variation induced perspective effect also introduces error. Errors like these may be negligible for slightly curved surfaces but must be taken into consideration for cylindrical or conical surfaces with small radii.

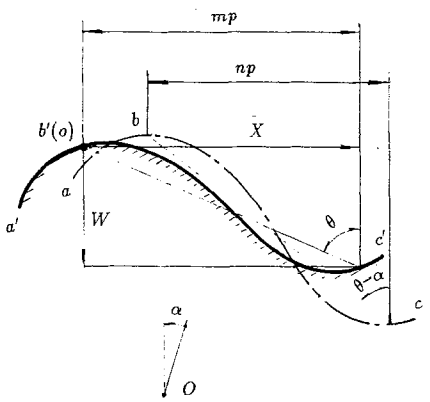

Fig. 4—Rotating the specimen about an arbitrary point

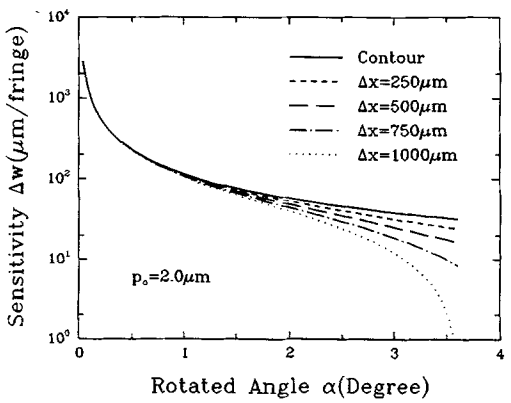

Fig. 5—Sensitivity versus rotated angle at various fringe spacings

In order to reduce this kind of error, a so called periphery camera[11] may be used for fringe-pattern recording on cylindrical, conical or near cylindrical, near conical surfaces. A periphery camera is capable of developing the circumference of a cylindrical or a conical surface into a plane. In doing so, x in the above expressions will be replaced by another variable l which is a direct measure from the fringe pattern photographed by the periphery camera. For a cylindrical surface, $l = R\phi$, $x = R\sin\phi$ and $\sin\phi = \sin(l/R)$. Thus, eq (15) can be rewritten in terms of l as

$$w = \frac{Np_0 - R\sin(l/R)(1-\cos\alpha)}{\sin\alpha} \tag{16}$$

In the following discussion, all the fringe patterns were recorded by such a periphery camera.

Further Discussion

Equations (12), (13) and (16) describe fringe equations for the topographic contours instead of contours because they are dependent on the x coordinate. They represent contour only if the second terms in the numerators are negligible compared with the first terms Np_0 yielding

$$w = \frac{Np_0}{\sin\alpha} \tag{17}$$

As shall be seen, such an approximation is valid for small rotating angles and small fringe spacing.

The sensitivity of this technique is determined by the difference in w between two adjacent fringes. Taking eq (15) as an example, the sensitivity is given by

$$\Delta w = w(N+1) - w(N) = \frac{p_0 - \Delta x(1-\cos\alpha)}{\sin\alpha} \tag{18}$$

where Δx is the difference in x between two adjacent fringes (fringe spacing in the X direction).

Apparently, p_0 and α all influence the sensitivity. Pitch p_0 is normally about the order of micrometer and takes a fixed value once the optical arrangement is fixed. Then the most easily adjustable factor is angle α. Figure 5 shows the relation between Δw (logarithmic scale) and α numerically calculated according to eq (18) where the grating pitch p_0 is taken to be 2.0 μm. The solid line represents the sensitivity for w contour [eq (17)] defined as

$$\Delta w = \frac{p_0}{\sin\alpha} \tag{19}$$

The sensitivity Δw evaluated for different values of fringe spacing Δx is also plotted in Fig. 5. It is seen that for small α values the sensitivity is almost independent of Δx. When $\alpha \leq 1$ deg, for $\Delta x \leq 1$ mm, the error in sensitivity caused by using contour expression [eq (19)] instead of topographic contour expression [eq (18)] is less than eight percent.

Figure 5 also shows that the sensitivity can be adjusted to the order of micrometer by making the rotation angle be about 3.5 deg for $\Delta x = 1$ mm. The lower limit of the

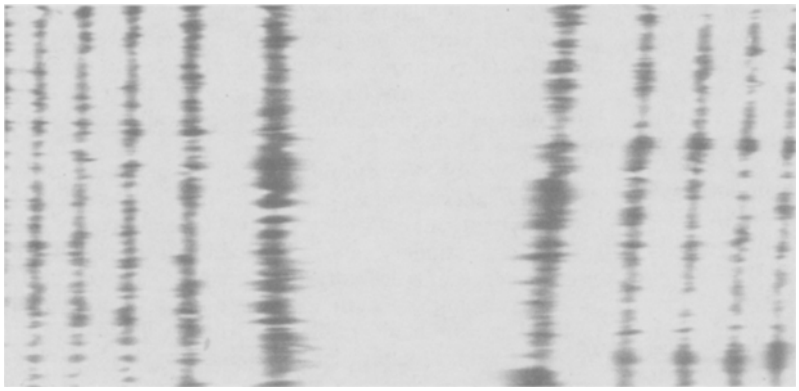

(a)

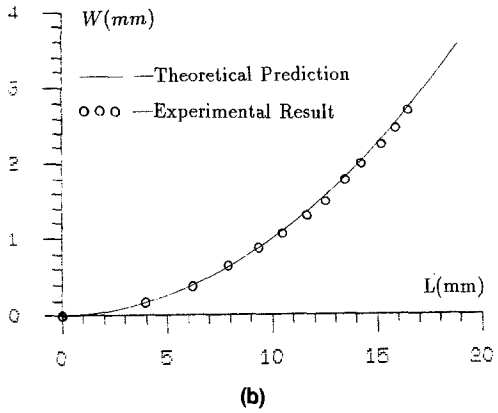

(b)

Fig. 6—Topographic contour study of a cylinder. (a) Topographic contour fringe pattern (R = 25.4 mm, p_o = 0.7 μm, α = 0.17 deg); (b) comparison

sensitivity, as shown in Fig. 5, can go as much as a few millimeters for sufficiently small angle rotations.

Equation (15) can be rewritten as

$$w = N\frac{p_o - (1-\cos\alpha)x/N}{\sin\alpha} \tag{20}$$

where x/N is the average fringe spacing. Noting that eq (20) is analogous to eq (18), we can conclude that Fig. 5 and the result of the above error analysis discussion can be readily applied to the comparison between topographic contour [e.g., eq (16)] and w contour [eq (17)] as well. Thus, the fringes obtained by the present technique approximately represent contours of equal w coordinates for small angle rotations ($\alpha \leq 1$ deg).

For a flat plane, Δw is zero and $p_o = p\cos\alpha$, eq (18) becomes

$$\Delta x = \frac{p_o}{1-\cos\alpha} = \frac{p_o p}{p - p_o} \tag{21}$$

This is exactly the same as the expression for fringe-spacing evaluation of a mismatch fringe pattern of classic moiré method.[10]

Experimental Investigation

The validity of the above derivation was verified by some experiments carried out on cylindrical shells with and without diametrical loading. The specimens were prepared according to a procedure described elsewhere[12] except that no aluminum coating was applied to the present work.

Figure 6(a) (R = 25.4 mm, p_o = 0.7 μm, α = 0.17 deg, Δw = 230 μm) is the fringe pattern of a uniform cylinder recorded by a periphery camera where the horizontal axis is no longer x but rather arc length l. The small circles in Fig. 6(b) are w coordinates calculated by eq (16) based on the fringe pattern obtained [Fig. 6(a)]; while the solid line represents w coordinates calculated according to the measurement of shell geometry by

$$w = R(1-\cos\theta) \tag{22}$$

Apparently, the experimental results agree well with the calculated one.

Figures 7 and 8 show some experimental results for nonuniform cylindrical shells. Figure 7 is the moiré fringe pattern of a cylindrical shell with some initial imperfec-

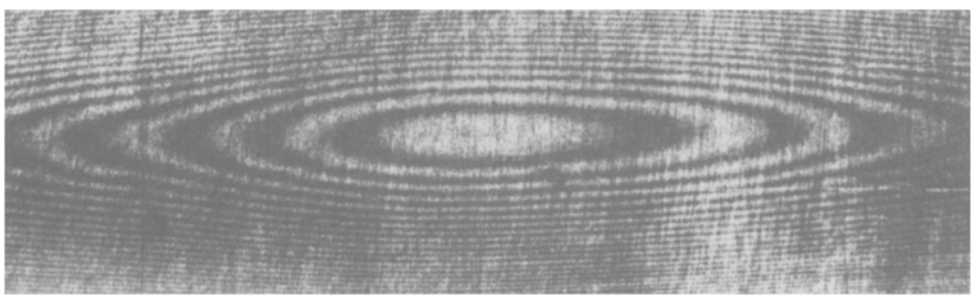

Fig. 7—Topographic fringe pattern of a shell with some imperfection

tion. Figure 8(a) (R = 50.2 mm, p_o = 1.66 μm, α = 0.6 deg, Δw = 157 μm) is the fringe pattern of a shell under diametrical point loading.

Applying this double-exposure moiré-interferometry technique twice, once before and once after a specimen is deformed, one will get two sets of moiré fringe patterns respectively. Comparing these two, one can find the w displacement due to the load alone. Figure 8(b) is such a comparison where the dots represent the w coordinates of a shell with the diametrical load and the solid line represents that without. The difference in w gives the displacement due to the loading alone. Therefore, surface-topographic contour or w displacement, no matter it is uniform or not, may be measured by double-exposure moiré interferometry.

Conclusion

An experimental technique, along with some theoretical derivation and experimental verification, for the determination of topographic contour, or contours of equal w coordinates for small angle rotations, based on a double-exposure moiré-interferometry technique, is presented. Its applications to the accurate determination of shell uniform radial deformation and of topography of arbitrarily curved surfaces are demonstrated.

The sensitivity of the technique is shown to be from the order of micrometers to that of millimeters. It can be easily adjusted by controlling the amount of rotation of the specimen relative to the optical system between the two exposures. Within a certain rotating limit, which is about four deg for the test conditions in the present work, the larger the rotated angle, the higher the sensitivity and *vice versa.*

The w evaluation expression is independent of the rotating object and its rotating center between the exposures. However, the change in rotating direction or the side of the X axis will alter the sign of a term in the expression. This difference is negligible for small angle rotations.

The fringe pattern produced by this method in general yields surface-topographic-contour because the coordinate x is involved in the expressions for the w coordinate evaluation. However, for very small angle relative rotations, this involvement is negligible indicating that the moiré fringes obtained by this technique represent contours of equal w coordinates.

The major drawback of this technique is that sometimes it is difficult to record the fringe pattern with the same contrast on the whole specimen surface because of the grating diffraction effect. Besides, *in situ* adjustment of fringe density such as that of the shadow moiré method is not possible with the present technique. This means that either a rough knowledge about the curved surface or a trial and error process is needed before a satisfactory fringe pattern can be obtained.

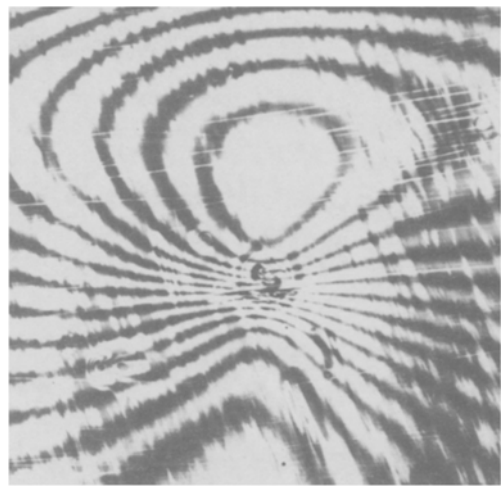

(a)

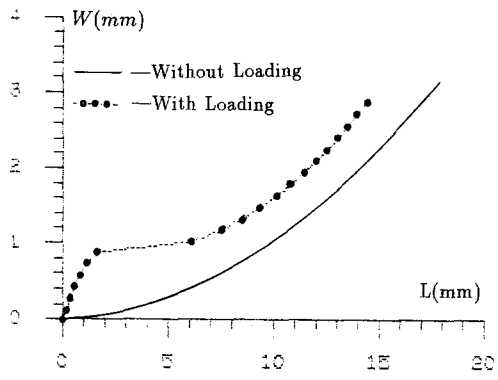

(b)

Fig. 8—Topographic contour study of a shell under diametrical loading. (a) Topographic contour fringe pattern (R = 50.2 mm, p_o = 1.66 μm, σ = 0.6 deg); (b) comparison

Acknowledgments

Financial supports provided by the Office of Naval Research, Solid Mechanics Division through contract No. N0001482K0566, and Army Research Office, Engineering Science Division through contract No. DAAL0388K0083 are acknowledged.

References

1. Dai, Y.Z. and Chiang, F.P., "Moiré Interferometry Applied to Topographic Contour Measurement," Proc. SPIE, **954**, *153-159 (1988).*

2. Meadows, D.W., Johnson, W.O. and Allen, J.B., "Generation of Surface Contours by Moiré Patterns," Appl. Opt., **9** *(4), 942-947 (1970).*

3. Takasaki, H., "Moiré Topography," Appl. Opt., **9** *(6), 1467-1472 (1970).*

4. Khetan, R.P., "Theory and Application of Projection Moiré Methods," PhD Thesis, State University of New York at Stony Brook (1975).

5. Hildebrand, B.P. AND Haines, K.A., "Multiple-Wavelength and Multiple-Source Holography Applied to Contour Generation," J. Opt. Soc. of Amer., **57** *(2), 155-162 (1967).*

6. Jaisingh, G.K. and Chiang, F.P., "Contouring by Laser Speckle," Appl. Opt., **20** *(19), 3385-3387 (1981).*

7. Post, D., "Development in Moiré Interferometry," Opt. Eng., **21** *(3), 458-467 (1982).*

8. Basehore, M.L. and Post, D., "Moiré Method for In-plane and Out-of-plane Displacement Measurement," EXPERIMENTAL MECHANICS, **21** *(9), 321-328 (1981).*

9. Beranek, W.J. and Bruinsma, A.J.A., "Determination of Displacement and Strain Fields Using Dual-beam Holographic-moiré Interferometry," EXPERIMENTAL MECHANICS, **20** *(9), 317-323 (1982).*

10. Chiang, F.P., "Moiré Methods of Strain Analysis," Manual on Experimental Stress Analysis, Third Edition, Chapt. 6, SESA, 51-69 (1979).

11. Chiang, F.P., Juang, R.M. and Dai, Y.Z., "Application of Moiré and Speckle Techniques to Curved Surfaces Using a Periphery Camera," Proc. SPIE, **814**, *249-256 (1987).*

12. Anastasi, R.F., Dai, Y.Z. and Chiang, F.P., "Simplified Procedure for Obtaining High-Frequency, Highly Reflective Specimen Gratings for Moiré Interferometry," EXPERIMENTAL TECHNIQUES, **12** *(9), 16-17 (1988).*